Fundamental Research on Deep Bed Filtration of Metals

Dipl.-Ing. Bettina Hübschen*, Prof. Dr.-Ing. Joachim Krüger, Prof. Dr.-Ing. W. Schneider**

IME, Institut für Metallurgische Prozesstechnik und Elektrometallugie, RWTH Aachen

Intzestr. 3;

52070 Aachen, Germany

* now McKinsey & Co, Düsseldorf

**Hydro Aluminium, Bonn

1 Introduction

Increasing demands on metal quality have led to the fact that filtration is a standard operation in aluminium foundries. Ceramic foam filters and classical deep bed filters are commonly used. By now, there is no theoretical platform describing deep bed filtration mode comprehensively. Working conditions for filters are only based on empirical data. The aim of this work is to describe mechanisms that occur inside ceramic foam filters in general. Two types of water models are used to achieve this: a full-scale model of an actual filtration box and a one-channel model that simulates one channel in a ceramic foam filter. For comparison also a deep bed filter is tested.

Especially flow velocity is crucial for the performance of a filter since this parameter allows particles to be deposited and retained inside the filter but also causes detachment of particles. Furthermore it is found that at flow velocities, which are applied in practical use, there are already turbulent conditions predominant in large parts of the filter. In these areas particles may not be deposited nd already detached particles can be washed out. Even singular perturbations like vibrations or uneven metal flow can cause particle detachment. Optimal and even flow conditions are therefore required for high filtration efficiency.

2 Filtration Through CFF

During deep bed filtration the inclusion are removed from the liquid/melt inside the filter. These particles are significantly smaller than the filter and this results in a high sensibility against hydrodynamic perturbations [1]. The liquid flows through the filter pores and the inclusions will attach to the pore walls in case of a CFF or the particles forming the filter for classical deep bed filters. These filters have been known for a long time already and have been used mainly in drinking water purification. There have been several developments especially for metal filtration. In the case of a classical deep bed filter, the particles are made of Al_2O_3. Besides this filter type, there are two more systems, which are also categorized in the filtration mode of deep bed filtration though they can be considered a "negative" of the classical type: the bonded particle tube filters (BPF) and the ceramic foam filters (CFF). BPF consist of very fine bauxite or SiC tubes. CFF are made of porous ceramic foam, Al_2O_3 in most cases. They are seen as the negative of a bed filter because the melt is not flowing around the particles of the filter but is running through its pores while the impurities are attached at the walls of these pores (figure 1) [2]. The specific surface of CFF and DBF are approximately the same if particles and pores are of the same size. However, there is a significant difference in open porosity with DBF showing values of about 0.4 while this is about twice as much for CFF with values reaching 0.8. [2]. This as a consequence results in very different flow regimes, as illustrated in figures 1. So the models used for evaluating flow conditions in DBF are only of limited use in the case of filtration through CFF. Already inside one pore of a CFF the flow conditions reach from laminar to turbulent, with zones of dead volume being present in most of the cases (figure 2). Both flow conditions and the conditions for particle attachment are different in both filter types.

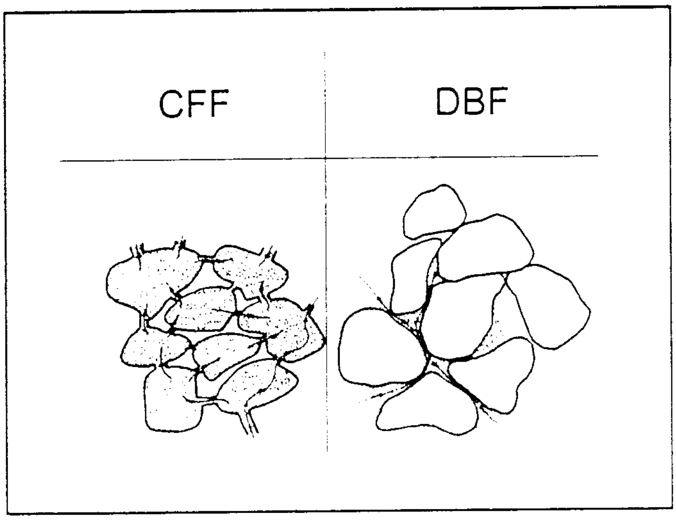

Figure 1: Flow regime in a CFF and DBF [3]

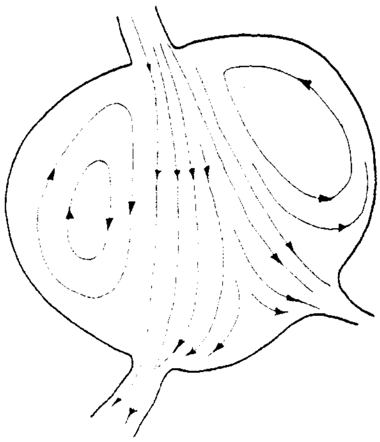

Figure 2: Flow conditions within one pore of a CFF [3]

Niedzinski et al. [4] were among the first to look at the flow conditions of an aluminium melt and the conditions for attachment of particles in a CFF resulting thereof (figure 3). It is obvious that particles are attached in the regions of the filter characterized by laminar flow conditions. The concentration of particles removed decreases with filter depth increasing. Also, increasing filter height, decreasing pore size and decreasing flow velocity have a positive effect on filtration efficiency.

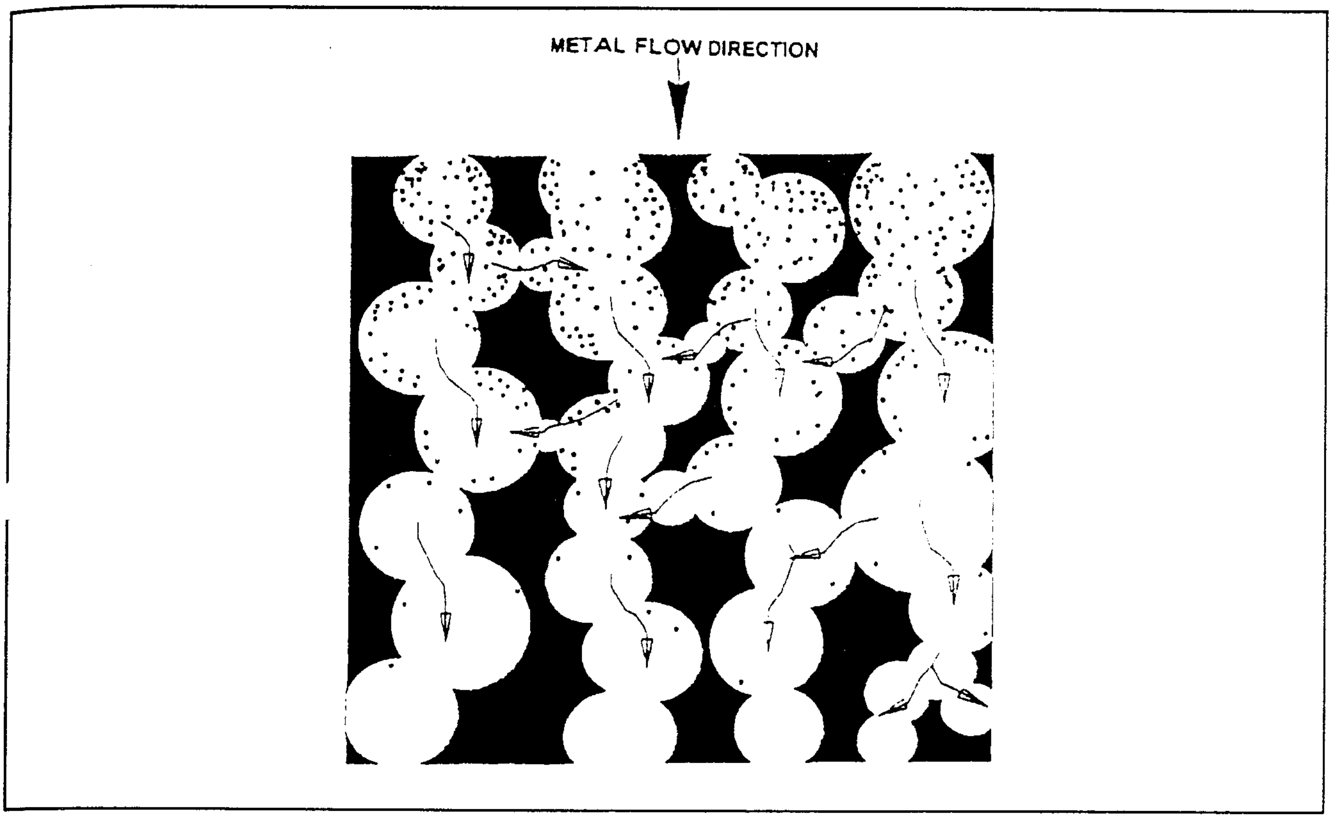

Figure 3: Attachment of particles in a CFF [4]

2.1 Influence of flow velocity

Flow velocity is a crucial parameter for filtration efficiency. If it is too high, it can cause release of already attached particles from the filter. But also vibrations, perturbations and unequal metal flow c have negative effects as can be seen from figure 4 showing values from actual metal filtration tests [5].

It is therefore important to understand the processes and mechanisms occurring inside the filter. It is assumed that the main force causing release of particles from the filter is the drag force of the liquid. The size of this force is direct proportional to the velocity of the melt (Stoke's Law) [2]. Filtration efficiency decreases with increasing flow velocity. For creating guidelines for the proper use of filters and application of appropriate flow velocity, it is therefore necessary to investigate the rheological aspects of metal filtration [2].

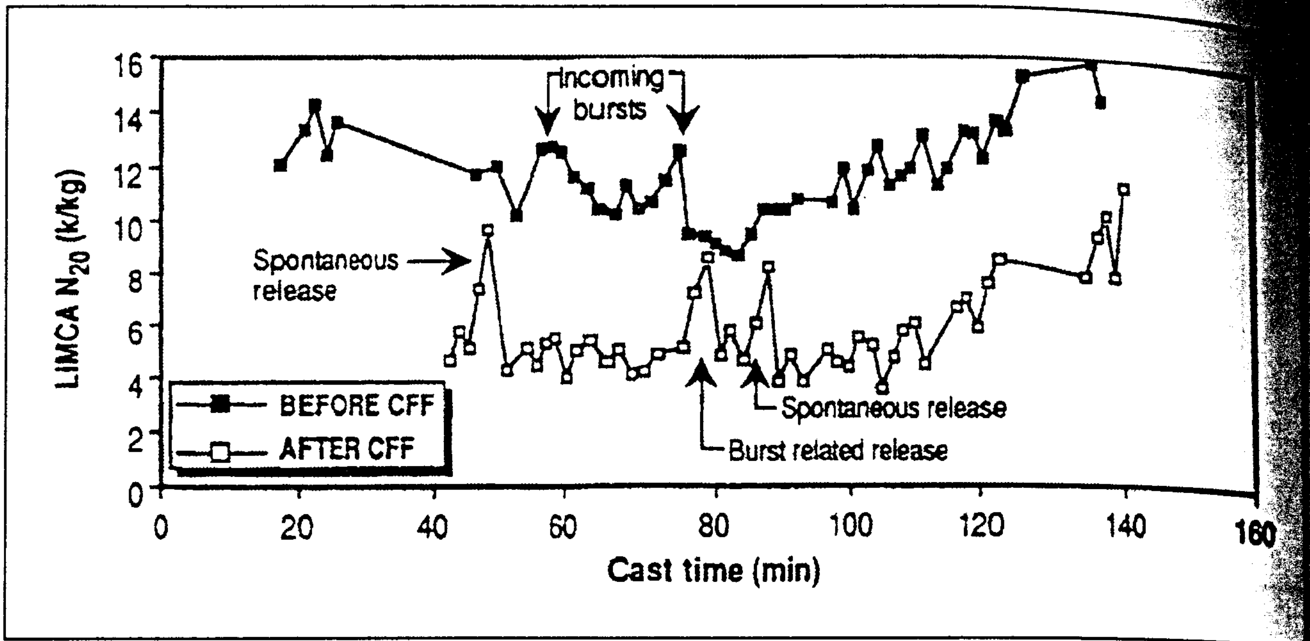

Figure 4: Release of particles from the filter after perturbations in the filtration process [5]

Pressure drop through a porous bed is described by the Ergun equation.

$$\frac{\Delta P}{H} = \frac{150 \cdot \mu \cdot u}{d_p^2} \cdot \frac{(1-\varepsilon)^2}{\varepsilon^3} + \frac{1{,}75 \cdot \rho \cdot u^2 \cdot (1-\varepsilon)}{d_p \cdot \varepsilon^3} \tag{1}$$

The first part is defining the influence of laminar flow, the second that of turbulent flow. At laminar flow conditions the equation can be simplified to:

$$\frac{\Delta P}{H} = \frac{150 \cdot \mu \cdot u}{d_p^2} \cdot \frac{(1-\varepsilon)^2}{\varepsilon^3} \tag{2}$$

This equals the Darcy equation that is valid for viscous flow of a Newtonian liquid flowing through a porous media.

Under laminar flow conditions, pressure drop will increase linearly with increasing flow velocity. If turbulent conditions are dominant, this linear correlation is no longer given. Guthrie found evidence that already at flow conditions practically applied turbulent conditions occur. In that case release of particles from the filter is likely. Usually superficial velocities are used for indication of flow velocities. However, real velocities are higher, yet changing rapidly at different locations inside the filer. The actual values of these real velocities are not known. An appropriate means to measure and determine the flow conditions in reactors are tracer measurements. /6/

3 Tracer Measurements

The CFF can be regarded as a continuous reactor and the different volume fractions can be determined to characterize the flow behavior inside the filter. One important characterization of the fluid flow is the average residence time, which is given by equation 3 [6] Instead of metals model substances are commonly used to simulate the flow, which allow measurements, which are easier and more exact and can easily be evaluated. Aqueous solutions are proven to be appropriate especially for the simulation of liquid aluminium and they allow easy tracer measurements, e.g. the change of electrical conductivity caused by a tracer liquid is an indicator for flow conditions that can be measured in real time.

$$\bar{t} = \frac{\text{volume of fluid in the vessel}}{\text{volumetric rate of fluid flow}} = \frac{V}{\dot{v}} \qquad (3)$$

where : $\bar{t}$ average residence time

V: volume of fluid in the vessel

$\dot{v}$: volumetric rate of fluid flow

Usually the residence time in reactors differs from the calculated residence time and a variety of different residence times can be found. This means that some fluid elements spend a longer and others a shorter period of time in the system. This distribution of residence times is an important characteristic and describes the performance of a reactor.

Tracer measurements are a tool to investigate the flow behavior. There are several methods for introducing tracer material into a system of which pulse input of tracer was used in this work. This involves the feeding of a quantity of tracer over a short time period into the system. The tracer material must not interact with the fluid in the reactor or the reactor itself and the amount of tracer has to be negligible in comparison with the amount of fluid present in the system. In addition the time period over which the tracer is introduced to the system has to be very small compared to the calculated residence time. The concentration of the tracer in the outlet stream is measured and plotted against time. The results can be plotted in dimensionless and therefore more general form by using specific variables (C-Diagrams) [6]:

$$C = \frac{c}{Q/V} \qquad (4)$$

where Q = quantity of tracer injected

V = Volume of fluid in the vessel

C = dimensionless exit concentration

And

$$\Theta = \frac{t}{\bar{t}} \tag{7}$$

where: Θ = dimensionless time

t = actual time

$\bar{t}$ = average residence time

The area under each C curve must be unity since the entire tracer introduced to the system must eventually leave the system [6].

$$\int_0^{\infty} C d\Theta = 1 \tag{8}$$

According to the distribution of residence times it is possible to define different reactor types of which the C Diagrams have a typical design. This is to be seen in figure 5.

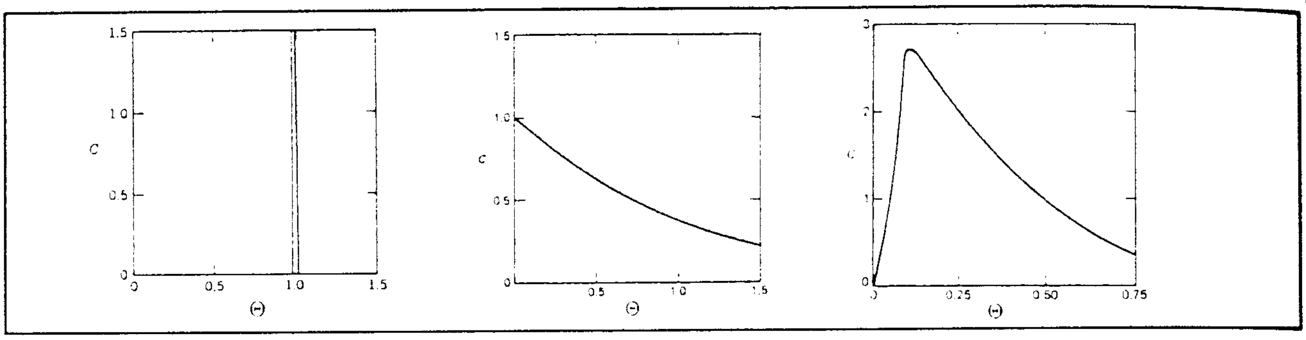

Figure 5: Basic reactor types: left: plug flow, middle: back mix flow, right: presence of dead volume [6]

In the case of plug flow the tracer elements introduced to the system do not mix at all while they pass the reactor and arrive at the outlet exactly at Q = 1. So there is no spread of residence time. (figure 5, left). In a back mix flow reactor the tracer is dispersed immediately and uniformly throughout the system. This means the tracer concentration in the outlet stream is equal to the concentration inside the reactor. Thus the C diagram shows a decrease in tracer concentration starting from unity during the test run. This means that a fraction of the tracer stays inside the system for a time much longer than expected while another fraction passes the system much faster (figure 5, middle). The presence of dead volume regions is indicated by a maximum in the C diagram at a time smaller than the average residence time and C > 1 (figure 5, right). The volume of the reactor seems to be much smaller than it actually is. Real reactors usually are a mixture of plug flow, back mix and dead volume. The C diagram for such a mixed model is shown in figure 6. The volume fractions can be determined from the diagram [6].

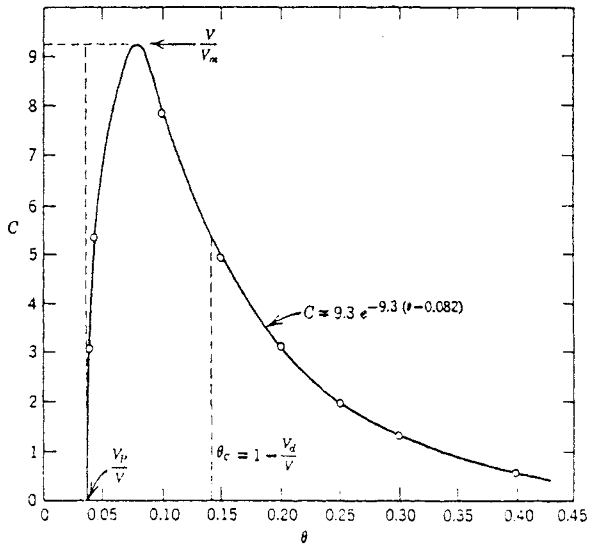

Figure 6 Determination of the volume fractions in a mixed model [6]

While in most cases dead volume decreases the performance of a reactor, for filtration a certain amount of dead volume seems to be essential for the deposition of particles.

4 Results

For the test work two different model types were used. The first one was a full-scale filter box model. Tracer tests on real CFF were made to investigate the change of flow behavior with the flow rate and filter pore size. The second water model type used was a specially designed single channel model to simulate the flow in one channel of a CFF. Three different single channel models were tested to investigate the influence of pore shape and flow direction on the flow behavior.

The setup of the models used for the investigations is shown in figure 7.

For all tests sulphuric acid was used as tracer and also $KMnO_4$ was added for visualization of the flow. A small amount of tracer was added at the inlet of the filter/model and an electrode at the outlet measured the electric conductivity, which gives an immediate signal for any change in concentration. A computer recorded the signal and thus the concentration-time-curve could be plotted. A valve in the outlet stream allowed different flow rates to be adjusted.

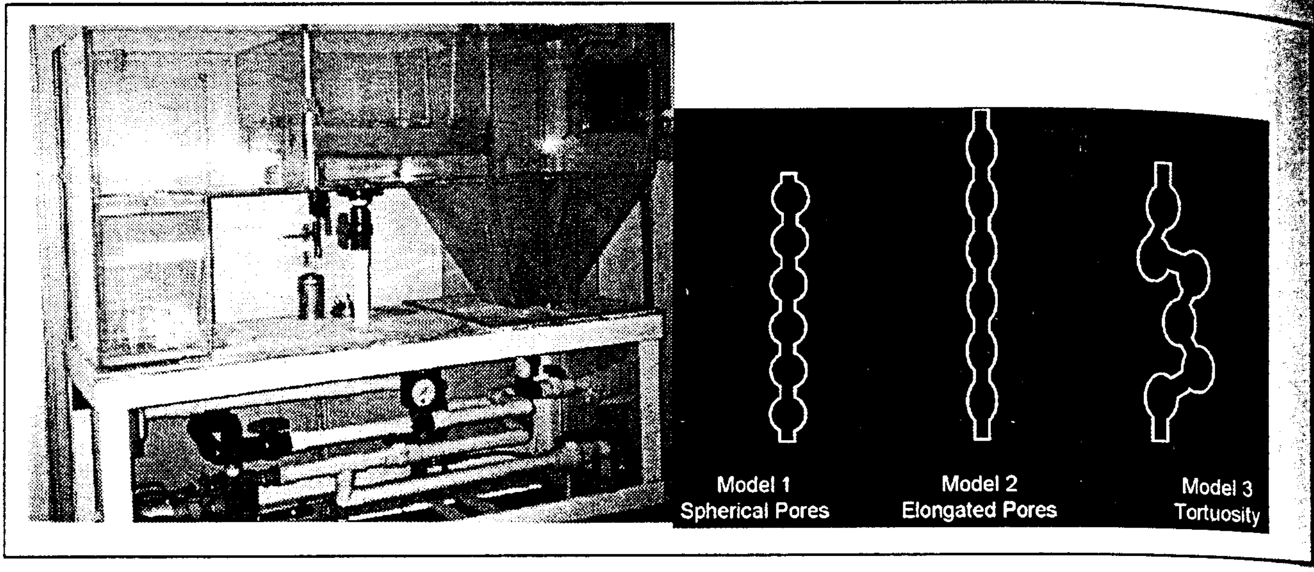

Figure 7 Water models used: Full-scale filtration box model (left), one-channel models (right)

4.1 Pressure Drop Measurements in Full Scale Model

As explained above the Ergun equation gives the correlation between pressure drop and flow velocity. It is also possible by the means of this equation to distinguish between pressure drop caused by laminar and by turbulent flow conditions. At laminar flow conditions, particle detachment and release from the filter should not occur, however at turbulent conditions, the chance for this increases. In order to evaluate the transition point from laminar to turbulent flow, the full-scale model was used to perform such pressure drop measurements. At a certain flow velocity the pressure drop was measured in the form of the difference of water level in front of and after the filter. Then the flow velocity was increased, the measurement repeated until the pressure drop over a whole range of flow velocities was recorded. This was executed for filters of different pore sizes. Both flow velocity and pore size proved to be important factors. For the 30 ppi filter a steady linear increase over the whole range of flow velocities was found, whereas for a 80 ppi filter the transition point from laminar to turbulent flow could be measured. The measured values were than compared with calculated values according the Ergun equation. As for velocity, superficial velocity divided by porosity was used, filter thickness was used for length L; the tortuosity factor of the liquid through the filter was not yet acknowledged, so real velocities will still be higher locally in the filter. Figure 8 shows measured and calculated values for a 30 ppi filter, figure 9 for an 80 ppi filter.

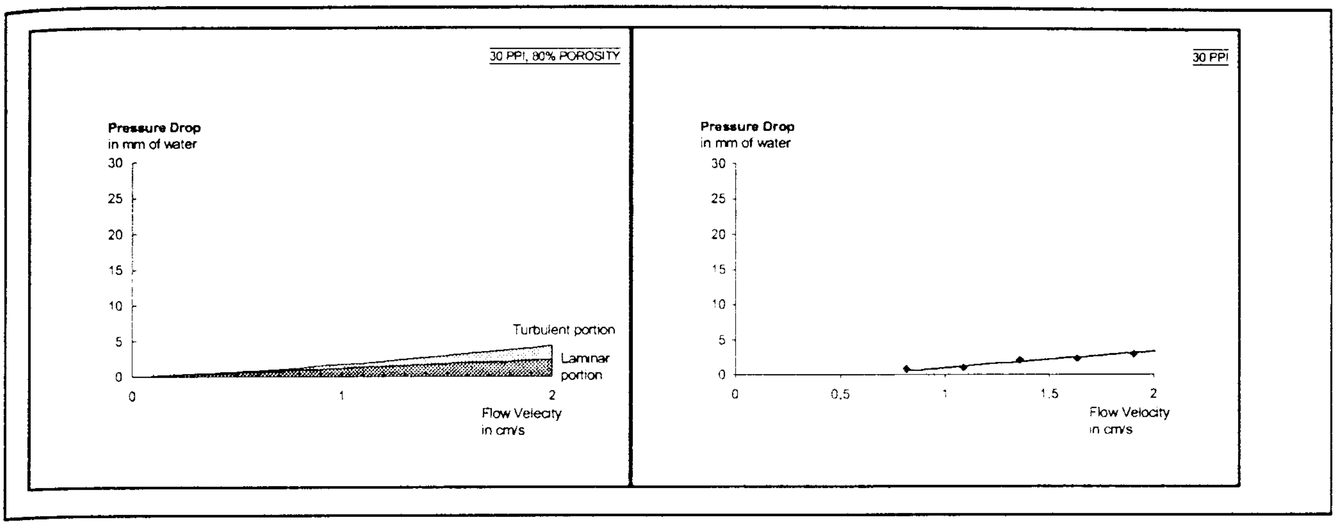

Figure 8: Calculated (left) and measure (right) pressure drop for a 30 ppi CFF filter

The measurements did not allow showing the transition point from laminar to turbulent flow. The overall pressure drop was low throughout the test range though, so tolerances of measurement accuracy would not allow noting a break in the linearity. But also the calculated values show that the influence of turbulent flow is indeed low for this filter. For the 80 ppi filter a clear transition from laminar to turbulent conditions could be measured. This also matches very well with the calculated values. It can also be noticed that the calculated values are slightly higher than the measured ones. This indicates that real velocities in the filter are higher than assumed. So the 80 ppi filter is operated at flow velocities where turbulent flow is predominant.

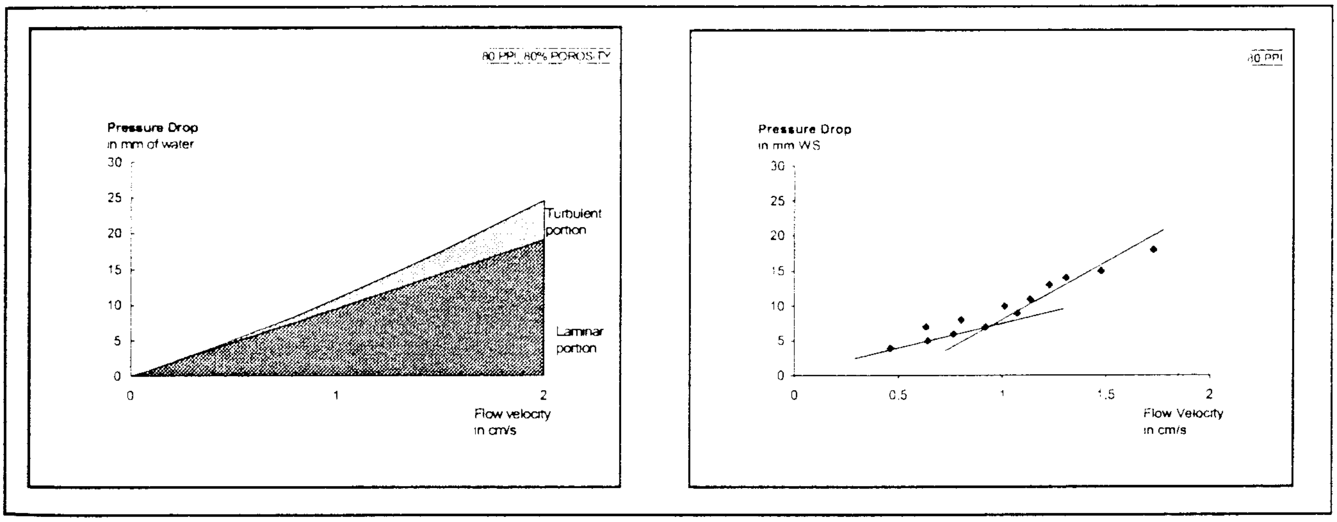

Figure 9: Calculated (left) and measure (right) pressure drop for an 80 ppi CFF filter

4.2 Tracer Measurements in Full Scale Model

For this test series, a certain flow rate was adjusted and then tracer introduced to the system directly on top of the CFF. The time for the first tracer to leave the filter at the bottom of the CFF was measured and compared to theoretical residence time. This was repeated over a range of flow velocities and for different CFF types. It was found that the measured time was significantly lower than the calculated time, indicating that real velocities are higher than theoretical ones but also indicating the presence of dead volume. As an example the results for a 30 ppi filter are shown in figure 10. For this type of measurement, only the time for the first tracer to leave the filter was measured. So only the presence of dead volume could be concluded from the results, however an exact breakdown of flow conditions could not be calculated. For this reason, the one-channel models were developed

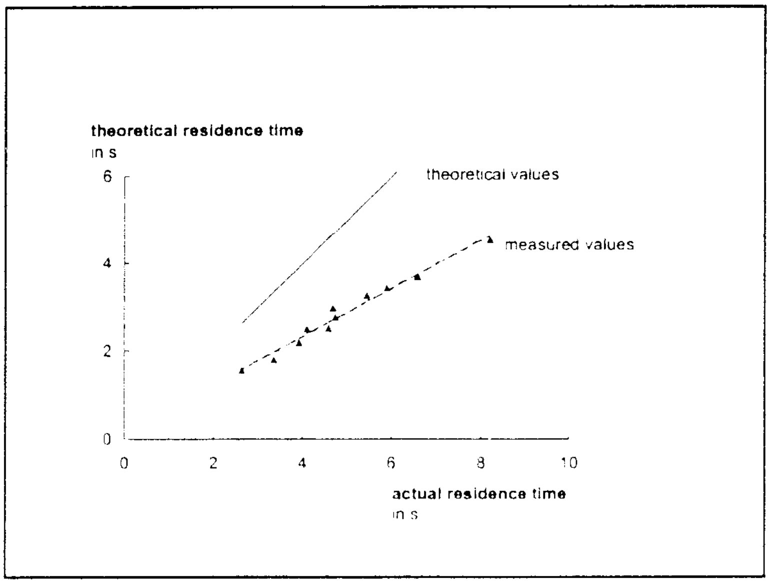

Figure 10: Theoretical and actual residence time inside a 30 ppi filter

4.3 Tracer measurements in one channel models

Three different shapes of models were used so that various parameters could be examined. The first model was characterized by round pores and a straight flow line for the liquid. In the second model the shape of the pores were elongated which represents a better model of the real filters. In the third model finally, also the fact was reflected that the liquid does not flow straight through the model but has to find its way through a tortuous way inside the filter (figure 7, right). In order to achieve similarity between the CFF and the one-channel models, the Reynolds numbers must be equal. Using the geometries of model and filter and taking into account that the model liquid was the same in CFF tests and one-channel tests, the correct flow velocities could be calculated.

$$\begin{aligned}
&Re_{CFF} = Re_{Mo} \\
&v_{Mo} = \frac{d_{CFF} \cdot v_{CFF}}{d_{Mo}} \\
&\Rightarrow v_{Mo_{max}} = 1{,}2\,mm/s \\
&\quad v_{Mo_{min}} = 0{,}14\,mm/s
\end{aligned} \tag{9}$$

The tracer was then introduced at the inlet of the one channel model; at the outlet an electrode measuring electrical conductivity was installed. By this set-up, a change in conductivity can be measured in real time and thus the concentration of tracer in the outlet is measured continuously. The results were plotted against time and this allowed so receive the C-diagrams as explained above. The tests were conducted at different flow rates, for each flow rate the breakdown of volume fractions calculated. So the change of flow behaviour as a function of flow velocity could be obtained. The results can be seen in the following figures.

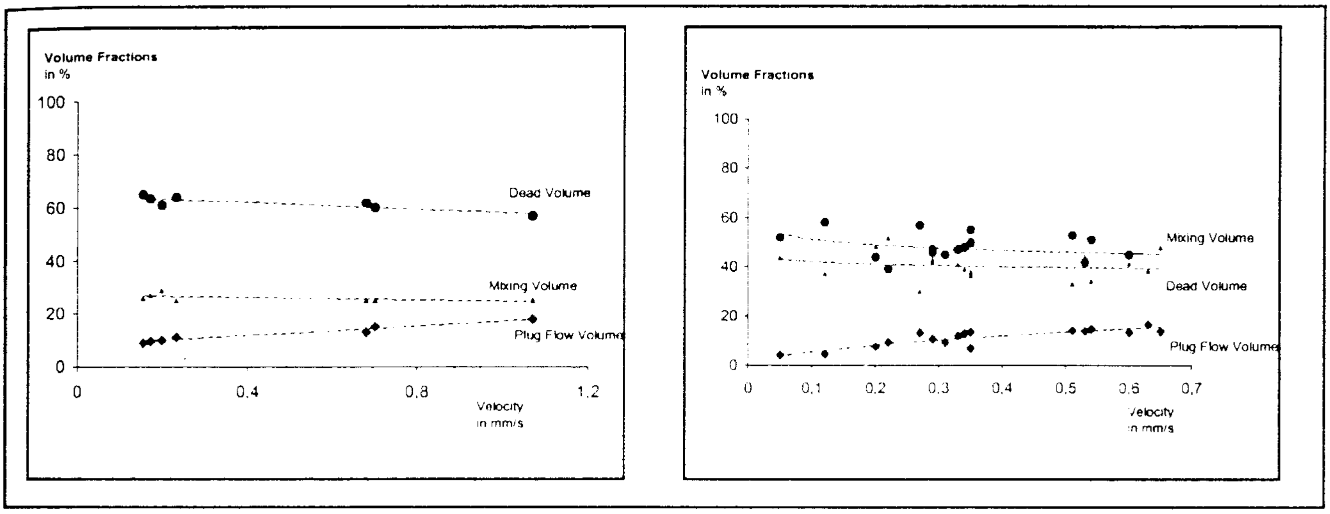

Figure 11: Volume Fractions in round-pore model (left) and elongated pore model (right)

Figure 11 shows the results for the round pore model and the elongated pore model; in figure 12 the results for the tortuosity model are shown. The following conclusions can be drawn for the results

- all three models showed decreasing dead volume parts if flow velocity increased

- at the same time all models showed increase in plug flow volume

- the round pore model had higher dead volume fractions than the elongated pore model

- at both the round pore and the elongated pore model, dead volume was evenly transformed into plug flow and mixing volume at increasing flow rates, at the tortuosity model however almost exclusively into mixing volume.

- at the elongated pore model and the tortuosity model, a sudden decrease of dead volume from a certain flow velocity could be observed. This shows again the sensibility of filtration against perturbations such as vibrations or uneven metal flow that cause a sudden increase in flow velocity

- at the tortuosity model the decrease of dead volume fraction started already at lower flow rates.

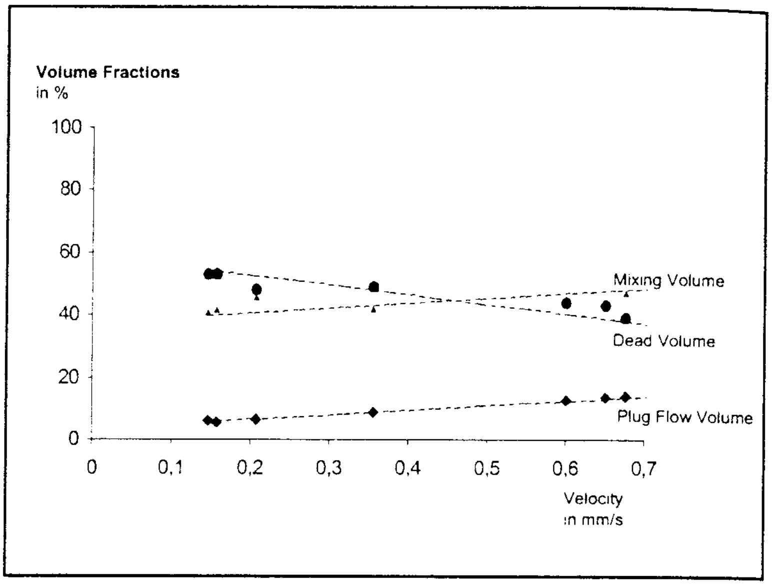

Figure 12: Volume fractions in tortuosity model

4.4 Tracer measurements in deep bed filter

To be able to compare the flow behaviour of CFF to those of classical deep bed filters, another model that simulated such a filter was used. The experimental set-up is shown in figure 13. The principles of measurement were analogue to the measurements at the one-channel models. Two grain sizes were used, one in a range of 2-4 mm, the second in the range of 4-8 mm.

The results showed that these deep bed filters feature a high percentage of dead volume at low flow rates. However with increasing flow velocity, the amount of dead volume decreased rapidly and very sudden from a certain flow velocity. Also, plug flow increase is negligible, with dead volume transforming into mixing volume almost entirely. If the grain size is finer, the dead volume fraction is smaller from the beginning with a continuous decrease at increasing flow velocities. Plug flow volume remains almost unchanged throughout the range of flow velocities. Figure 14 shows the results of these measurements.

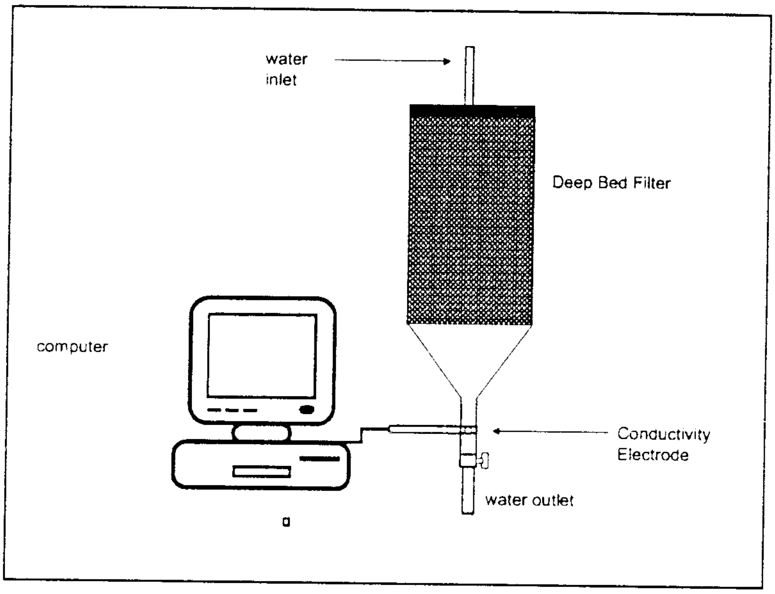

Figure 13: Set-up for deep bed filter measurements

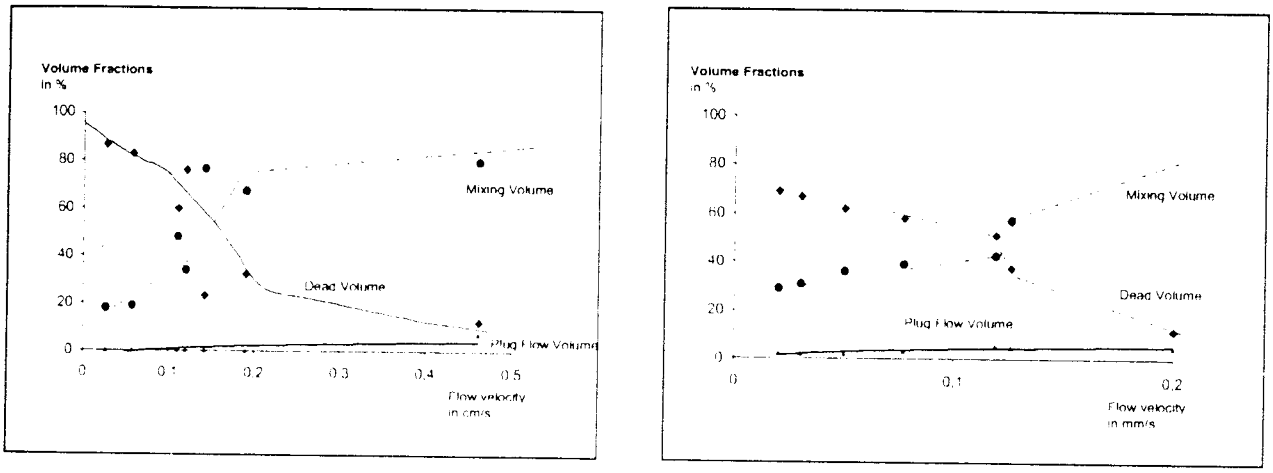

Figure 14: Flow behaviour of deep bed filters. Left: grain size 4-8mm, right: grain size 2-4 mm

4.5 Comparison of models

Table 1 shows a comparison of the most important results from the tortuosity one-channel model to the deep bed filters. Also Reynolds numbers in the laminar and turbulent flow regions were calculated. In the transition range from laminar to turbulent flow, Reynolds numbers in deep bed filter and one-channel model are very low, ranging from 2-5. The real velocity in the single pores of the filter however is supposed to be higher, thus also Reynolds numbers should show higher values already here. The value measured at the tortuosity model therefore reflects reality quite well. Though the Reynolds number does not indicate presence of turbulent flow conditions, the tracer measurement proved evidence that in parts of the filter turbulent conditions are indeed occuring. In all models dead volume changed into mixing volume at higher flow rates. The final value is sim for all models.

Given the fact that producers of CFF such as Pyrotek or Selee recommend operation of their fil in a range of 0,5 to 1,7 cm/s [7], [8] and taking into account that according to hydraulic analo (see table 2) Reynolds number in aluminium are twice as high at same flow velocity than in wat it is clear that already in the lower operating range filters are close to turbulent flow conditions.

Table 1: Comparison of deep bed filters with one-channel model

		One-channel model, tortuous	Deep bed filter 4-8 mm	Deep bed filter 2-4 mm
Window size*	cm	1,2	0,29	0,15
Superficial velocity at transition point laminar-turbulent	cm/s	0,13	0,15	0,12
Reynolds number at transition point		15,6	4,4	1,8
Laminar region**				
V_p	%	6	0	2
V_d	%	53	82	69
V_m	%	41	18	29
Transition region				
V_p	%	7	0	6
V_d	%	9	76	51
V_m	%	85	34	43
Turbulent range***				
V_p	%	20	7	5
V_d	%	3	13	12
V_m	%	77	80	83

* for deep bed filters, an equivalent diameter is calculated, derived from the volume around the filter particles; ** at low flow velocities;***at maximum flow velocity

Table 2: Hydraulic analogy water - aluminium for CFF for one flow velocity

		Aluminium	Water
Density	g/cm^3	2,345 (750°C)	1,0 (25°C)
Viscosity	mPas	1,13	1,0
char. Length L	cm	0,04	0,04
u_0	cm/s	0,61	0,61
u_w	cm/s	0,95	0,95
Re u_0	-	5,06	2,44
Re u_w	-	7,89	3,8

5 References

[1] DESMOULINS, J. P. (1992): Reliability of molten metal filtration -Light Metals 1992, S. 1101 - 1111

[2] TIAN, C.; GUTHRIE, R.I.L. (1993): Rheological aspects of liquid metal filtration using reticulated ceramic foam filters - Light Metals 1993, S. 1003 - 1007

[3] APELIAN, D.; MUTHARASAN, R.; ROMANOWSKI, C. A. (1982): Commercially available porous media for molten metal treatment - Light Metals 1982, S. 935 - 967

[4] NIEDZINKSI, M.M.; WILLIAMS, E.M.; SMITH, D.D.; AUBREY, L.S. (1999): Staged Filtration Evaluation at an aircraft plate and sheet manufacturer - Light Metals 1999, 1019 - 1030

[5] DUPUIS, C.; BÉLAND, G.; MARTIN, J.-P. (1993): Filtration Efficiency of ceramic foam filters for production of high quality molten aluminium alloys - Proceedings of the international symposium on light metals processing and application, Québec city, Québec, August 29-September 1, 1993, S. 349 - 358

[6] SZEKELY, J.; THEMELIS, N (1991): Rate Phenomena in Process Metallurgy; Wiley-Interscience, 1971

[7] Website Pyrotek company (www.pyrotek.com); Information paper on CFF

[8] Wesite Selee company (www.selee.com); Information paper on CFF